



Since January 2020 Elsevier has created a COVID-19 resource centre with free information in English and Mandarin on the novel coronavirus COVID-19. The COVID-19 resource centre is hosted on Elsevier Connect, the company's public news and information website.

Elsevier hereby grants permission to make all its COVID-19-related research that is available on the COVID-19 resource centre - including this research content - immediately available in PubMed Central and other publicly funded repositories, such as the WHO COVID database with rights for unrestricted research re-use and analyses in any form or by any means with acknowledgement of the original source. These permissions are granted for free by Elsevier for as long as the COVID-19 resource centre remains active.



A meta-analysis of comorbidities in COVID-19: Which diseases increase the susceptibility of SARS-CoV-2 infection?

Manoj Kumar Singh^{a,b,1}, Ahmed Mobeen^{a,b,1}, Amit Chandra^{a,b,1}, Sweta Joshi^c,
Srinivasan Ramachandran^{a,b,*}

^a CSIR-Institute of Genomics and Integrative Biology, New Delhi, 110007, India

^b Academy of Scientific and Innovative Research (AcSIR), Ghaziabad, 201002, India

^c Jamia Hamdard, Hamdard Nagar, New Delhi, 110062, India

ARTICLE INFO

Keywords:

COVID-19
Comorbidity
SARS-CoV-2
Leukemia
NAFLD
Psoriasis
Cancer
Type II diabetes

ABSTRACT

Comorbidities in COVID-19 patients often lead to more severe outcomes. The disease-specific molecular events, which may induce susceptibility to Severe Acute Respiratory Syndrome Coronavirus 2 (SARS-CoV-2) infection, are being investigated. To assess this, we retrieved array-based gene expression datasets from patients of 30 frequently occurring acute, chronic, or infectious diseases. Comparative analyses of the datasets were performed after quantile normalization and log₂ transformation. Among the 78 host genes prominently implicated in COVID-19 infection, *ACE2* (receptor for SARS-CoV-2) was positively regulated in several cases, namely, leukemia, psoriasis, lung cancer, non-alcoholic fatty liver disease (NAFLD), breast cancer, and pulmonary arterial hypertension (PAH). *FURIN* was positively regulated in some cases, such as leukemia, psoriasis, NAFLD, lung cancer, and type II diabetes (T2D), while *TMPRSS2* was positively regulated in only 3 cases, namely, leukemia, lung cancer, and T2D. Genes encoding various interferons, cytokines, chemokines, and mediators of *JAK-STAT* pathway were positively regulated in leukemia, NAFLD, and T2D cases. Among the 161 genes that are positively regulated in the lungs of COVID-19 patients, 99–111 genes in leukemia (including various subtypes), 77 genes in NAFLD, and 48 genes in psoriasis were also positively regulated. Because of the high similarity in gene expression patterns, the patients of leukemia, NAFLD, T2D, psoriasis, and PAH may need additional preventive care against acquiring SARS-CoV-2 infections. Further, two genes *CARBONIC ANHYDRASE 11 (CA11)* and *CLUSTERIN (CLU)* were positively regulated in the lungs of patients infected with either SARS-CoV-2, or SARS-CoV or Middle East Respiratory Syndrome Coronavirus (MERS-CoV).

1. Introduction

Coronavirus disease (COVID-19) caused by Severe acute respiratory syndrome coronavirus 2 (SARS-CoV-2) is the most dreaded pandemic of recent times. As per the global data released on December 25, 2020, by COVID-19 dashboard of the World health organization, SARS-CoV-2 has infected 77,920,564 people of which 1,731,901 people have died. A significant proportion of the COVID-19 patients have been reported to suffer from other pathophysiological conditions as well. For instance, in a cohort of 1590 COVID-19 patients from China, Guan et al. (2020) reported that 399 patients (25.1%) were having at least one comorbidity, while 130 patients (8.2%) had two or more comorbidities [1]. They reported that hypertension, diabetes, cardiovascular diseases, and

chronic kidney diseases were among the most frequent comorbidities, which occurred in 16.9%, 8.2%, 3.7%, and 1.3% of all COVID-19 patients, respectively. Also, COPD and malignancy were identified as critical risk factors associated with severe COVID-19 conditions. Another study by Chen et al. (2020) reported that in a cohort of 99 COVID-19 patients in China, 50 patients (51%) suffered from chronic medical illnesses [2]. The reported comorbid diseases were cardiovascular or cerebrovascular diseases (40.4%), diabetes (12%), digestive system disease (11%), and malignant tumor (0.01%) that were identified in 40, 12, 11, and 1 patient, respectively. Similarly, others have also reported cancer of lungs [3] and of blood [4], NAFLD [5], and HIV infections (Human Immunodeficiency Virus) [6], as frequently occurring comorbidities that often worsen the outcome and increase the risk of

* Corresponding author. 130, CSIR-Institute of Genomics and Integrative Biology, Mathura Road, New Delhi, 110025, India
E-mail address: ramu@igib.res.in (S. Ramachandran).

¹ Equally contributed.

mortality in COVID-19 patients.

Similarly Dolan et al. (2020) have reported comorbidities in severe forms of COVID-19 [7]. These included cardiovascular diseases, diabetes, hepatitis, lung disease, and kidney disease in addition to the previously mentioned comorbidities. However, the molecular mechanisms underlying COVID-19 associated comorbidities are poorly understood and are still being investigated. The aim of this study was to decipher such diseases and their associated gene expression patterns that may induce susceptibility to SARS-CoV-2 infection. We performed a meta-analysis with gene expression datasets in 30 widely prevalent acute, chronic, and infectious diseases to identify the gene expression signatures that could promote the pathogenesis of SARS-CoV-2. We found that the gene expression pattern in leukemia patients was most similar to SARS-CoV-2 cases, followed by the patients of chronic diseases, namely, non-alcoholic fatty liver disease (NAFLD), psoriasis, type II diabetes (T2D), and pulmonary arterial hypertension (PAH). Our study could serve as a guide for understanding the gene expression signatures underlying COVID-19 associated comorbidities.

2. Dataset, methods, and techniques

2.1. Data retrieval

Publicly available datasets of human acute, chronic, infectious diseases, and various types of cancer were retrieved from NCBI's GEO database [8]. We favored the expression profile GSEids with highest number of samples while focussing on the tissue of origin, and devoid of any treatments or other afflictions. We retrieved datasets of patients and controls for the following conditions: Asthma (GSE64913), Chronic Obstructive Pulmonary Disorder (COPD, GSE112811), Cardiovascular diseases (GSE109048), Hypertension (GSE113439), NAFLD (GSE49541, GSE107037), Atherosclerosis (Athero, GSE28829), T2D (GSE15653, GSE25462, GSE38642, GSE27949), Polycystic Ovary Syndrome (PCOS, GSE124226), Multiple Sclerosis (MS, GSE21942), Psoriasis (GSE78097), Blood Cancer or Leukemia (GSE51082, GSE9476), Breast Cancer (GSE65194), Cervical Cancer (GSE63514), Multiple Myeloma (MM, GSE85837), Lung Cancer (GSE136043), Lung adenocarcinoma or Non-small cell lung cancer (NSCLC, GSE118370), Liver Cancer (GSE88839), Pancreatic Ductal Adenocarcinoma (PDAC, GSE101448), AIDS (GSE73968), Tuberculosis (TB, GSE139825), Malaria (GSE119150), Acute Kidney Injury (AKI, GSE30718), and COVID-19 (GSE150316). In order to identify the common differentially expressed genes in different viral infections, we analyzed the datasets from the patients infected with either SARS-CoV (GSE1739), SARS-CoV-2 (GSE150316), MERS-CoV (GSE100496), H1N1 (GSE21802), or other influenza viruses (GSE22319; H7N1, H5N1, H3N2, H5N2). Furthermore, we studied six subtypes of leukemia that were retrieved from the GSE51082 and GSE9476 datasets, namely Acute myeloid leukemia (AML), B-cell chronic lymphocytic leukemia (BCLL), Chronic myelogenous leukemia (CML), Myelodysplastic syndrome (MDS), B-acute lymphoblastic leukemia (BALL), and T-cell acute lymphoblastic leukemia (TALL). The dataset on cardiovascular diseases included an equal number of patients suffering from coronary artery disease (CAD) and acute myocardial infarction (AMI), and the dataset of breast cancer included both breast cancer and triple-negative breast cancer tissues (TNBC) samples. Of the 29 samples in the GSE28829 dataset of atherosclerosis (Athero), 16 samples were from advanced atherosclerotic plaque (ATHERO-Adv), and 13 samples were from early atherosclerotic plaque (ATHERO-Early) regions. In the cases of leukemia and NAFLD, we obtained expression profiles of diseased and control samples from separate GSEids. Therefore, we used a data-integration strategy as previously explained by Hamid et al. (2009) for data analysis in leukemia and NAFLD cases [9,10]. The platform of microarray experiment, type of tissue sample, sample size, experimental design, and data processing strategy, are summarized in Table 1.

2.2. Data normalization

The datasets used in this study were all quantile normalized, and log₂ transformed in R [11]. Briefly, raw expression values were quantile normalized using the normalize Quantiles function of LIMMA package in R, irrespective of their normalization status to maintain uniformity [12]. Subsequently, the average expression value of all probes for each gene in all the disease and control samples was obtained using collapse Rows function of WGCNA R package [13]. The normalized values were subsequently log₂-transformed, provided the dataset was not already log₂-transformed.

2.3. Data analysis

Principal Component Analysis (PCA) is a dimensionality reduction technique that identifies patterns in data, and highlights their similarities and differences. Elucidation of the principal components is based on identifying the variables most strongly correlated with each component. We used 'prcomp' function in R base package for PCA to analyze the segregation of datasets based on linear correlation and variance in gene expression values of 10,296 genes for all subjects in each disease [14]. The 'ggbiplot' function of ggplot2 package in R was used for graphical representation of PCA results [15].

Literature mining was carried out to identify 78 genes, which includes those encoding receptors, proteases, and others that are implicated in the replication and pathogenesis of one or other human infecting coronaviruses including SARS-CoV-2. The fold change values in the expression of these genes were computed and used to generate a clustered heatmap using pheatmap R package [16]. In addition, another heatmap was prepared using the gene expression values of 182 differentially expressed genes (at fold change > 2 or < 0.5 and p < 0.05) in COVID-19 patients compared to healthy controls. We used student's *t*-test (p < 0.05 as the level of significance) to analyze the gene expression data from SARS-CoV-2 infected human lung tissue. Additionally, the p-adjusted values (FDR < 0.05) were used for identifying the highly significant dysregulated pathways in different disease cases. The data has been plotted as mean ± standard error from mean, and each dot represents individual reading. The graphical representation of gene expression values was obtained using GraphPad Prism (version 8.0.0) software. The overall methodology of this study is shown in Fig. 1 (Created with BioRender.com).

2.4. Co-expression analysis

Co-expression analysis describes the correlation pattern in gene expression across different samples and it is frequently used for identifying the clusters (or modules) of highly correlated genes. We have used the weighted gene correlation network analysis (WGCNA) technique using WGCNA R package for identifying the highly correlated modules [13]. For co-expression analyses of individual disease cases, we have used the quantile normalized log₂ values of gene expression in disease samples. For co-expression analysis of multiple diseases, we have used log₂(FC) values. To ensure a scale-free topology of the network, soft-threshold power (ranged between 6 and 10) was chosen as per the Power Estimate value provided by pickSoft Threshold function in WGCNA R package. The pathway analysis for the genes in the identified modules were performed using DAVID [17]. The networks were drawn using Cytoscape 3.8 [18].

STAR METHODS:

LEAD CONTACT: The relevant information and requests for resources should be directed to and will be fulfilled by the Lead Contact, Srinivasan Ramachandran (ramu@igib.res.in).

MATERIALS AVAILABILITY: This study did not generate any new material.

DATA AND CODE AVAILABILITY: This study did not generate any unique dataset or code.

Table 1
Details of Expression Datasets taken from GEO for the study.

Disease Type	Disease/Condition	GSE ID	Platform	Tissue	Experimental Design	Data Processing
Chronic	Asthma	GSE64913	GPL570 [HG-U133_Plus_2] Affymetrix	Epithelial brushings from central and peripheral airways	42 healthy volunteer, 28 asthmatic patients	Preprocessed: Normalization and log ₂ transformation by GCRMA method
	Chronic Obstructive Pulmonary Disorder	GSE112811	GPL570 [HG-U133_Plus_2] Affymetrix	Blood	20 COPD patients, 22 healthy volunteers before administration of LPS or saline	Preprocessed: Normalization and log ₂ transformation by RMA
	Cardiovascular	GSE109048	GPL17586 [HTA-2.0] Affymetrix	Blood platelets	19 Healthy donors, 19 CAD patients, 19 AMI patients	Preprocessed: SST-RMA normalization and log ₂ transformation
	Hypertension	GSE113439	GPL6244 [HuGene-1.0-st] Affymetrix	Lung	15 patients with Pulmonary Arterial Hypertension and 11 normal controls	Preprocessed: Normalization and log ₂ transformation by RMA
	Non-Alcoholic Fatty Liver Disease	GSE49541	GPL570 [HG-U133_Plus_2] Affymetrix	Liver	72 patients with NAFLD	Preprocessed: Normalization and log ₂ transformation by GCRMA method
		GSE107037	GPL570 [HG-U133_Plus_2] Affymetrix	Liver	33 healthy liver donors	Preprocessed: Normalization and log ₂ transformation by RMA
	Atherosclerosis	GSE28829	GPL570 [HG-U133_Plus_2] Affymetrix	Carotid artery	Samples from atherosclerotic carotid artery segments of 29 patients	Preprocessed: Normalization and log ₂ transformation by RMA
	Type 2 Diabetes	GSE15653	GPL96 [HG-U133A] Affymetrix	Liver	4 type 2 diabetes and 5 control subjects	Preprocessed: MAS5.0 signal intensity.
		GSE25462	GPL570 [HG-U133_Plus_2] Affymetrix	Muscle	10 subjects with type 2 diabetes and 15 healthy subjects	Preprocessed: MAS5.0 signal intensity.
		GSE38642	GPL6244 [HuGene-1.0-st] Affymetrix	Pancreas	54 non-diabetic and 9 diabetic cadavers	Preprocessed: Normalization and log ₂ transformation by RMA
		GSE27949	GPL570 [HG-U133_Plus_2] Affymetrix	Adipose	12 Normal and 11 T2D subjects	Preprocessed: Normalization and log ₂ transformation by RMA
		GSE124226	GPL570 [HG-U133_Plus_2] Affymetrix	Adipose	4 PCOS women and 4 control subjects	Preprocessed: Normalization and log ₂ transformation by RMA
	Multiple Sclerosis	GSE21942	GPL570 [HG-U133_Plus_2] Affymetrix	PBMCs	12 MS patients and 15 controls	Preprocessed: Normalization GCRMA method
	Psoriasis	GSE78097	GPL570 [HG-U133_Plus_2] Affymetrix	Skin	6 normal skin tissues and 27 psoriatic skin lesions	Preprocessed: Normalization GCRMA method
	Cancer	Blood Cancer (Leukemia)	GSE51082	GPL96 [HG-U133A] Affymetrix	Bone Marrow	37 AML, 41, BCLL1, 22 CML, 10 MDS, 17 B-ALL, 12 T-ALL
GSE9476			GPL96 [HG-U133A] Affymetrix	Bone Marrow	38 healthy donors	Preprocessed: Normalization and log ₂ transformation by RMA
Breast Cancer		GSE65194	GPL570 [HG-U133_Plus_2] Affymetrix	Breast sample	11 control breast sample, 98 breast cancer samples, 55 TNBC samples	Preprocessed: Normalization and log ₂ transformation by GCRMA method
Cervical Cancer		GSE63514	GPL570 [HG-U133_Plus_2] Affymetrix	Cervix	24 normal and 28 cancer specimens	Preprocessed: Normalization and log ₂ transformation by GCRMA method
Multiple Myeloma		GSE85837	GPL10558 Illumina HumanHT-12 V4.0	Bone Marrow	9 control and 9 multiple myeloma patients with bone lesion	Preprocessed: Robust spline normalization and log ₂ transformation by lumi R package
Lung Cancer		GSE136043	GPL13497 Agilent-026652	Lung	5 lung cancer tissue and 5 lung non-tumor tissues	Preprocessed: Normalization by Agilent Feature Extraction Software
Lung adenocarcinoma (Non-small cell lung cancer)		GSE118370	GPL570 [HG-U133_Plus_2] Affymetrix	Lung	6 invasive lung adenocarcinoma tissues and 6 normal lung tissues	Preprocessed: Normalization and log ₂ transformation by MAS5.0 algorithm
Liver Cancer		GSE88839	GPL570 [HG-U133_Plus_2] Affymetrix	Liver	35 HCA liver tumours and 3 normal liver samples	Preprocessed: Normalization by RMA
Pancreatic Ductal Adenocarcinoma		GSE101448	GPL10558 Illumina HumanHT-12 V4.0	Pancreas	18 with pancreatic tumor and 13 non-tumor pancreatic tissue samples	Preprocessed: Normalization and log ₂ transformation by Illumina's BeadStudio Data Analysis Software
Infectious		AIDS	GSE73968	GPL6244 [HuGene-1.0-st] Affymetrix	T Cells	9 healthy control and 6 HIV positive patients
	Tuberculosis	GSE139825	GPL10558 Illumina HumanHT-12 V4.0	Alveolar Macrophages	Alveolar Macrophages from 5 TB patients and 5 control subjects	Preprocessed: Normalization and log ₂ transformation by lumi R package
	Malaria	GSE119150	GPL15207 [Prime View] Affymetrix	Blood	6 falciparum malaria and 6 normal subjects	Preprocessed: Normalization and log ₂ transformation by RMA
Acute	Acute Kidney Injury	GSE30718		Kidney		Preprocessed: Normalization and log ₂ transformation by RMA

(continued on next page)

Table 1 (continued)

Disease Type	Disease/Condition	GSE ID	Platform	Tissue	Experimental Design	Data Processing
	COVID-19	GSE150316	GPL570 [HG-U133_Plus_2] Affymetrix GPL18573	Lung	28 transplants with AKI to 11 pristine protocol biopsies of stable transplants 16 lung samples with COV2 positive and 5 control lung samples	Preprocessed: DEseq2 normalized

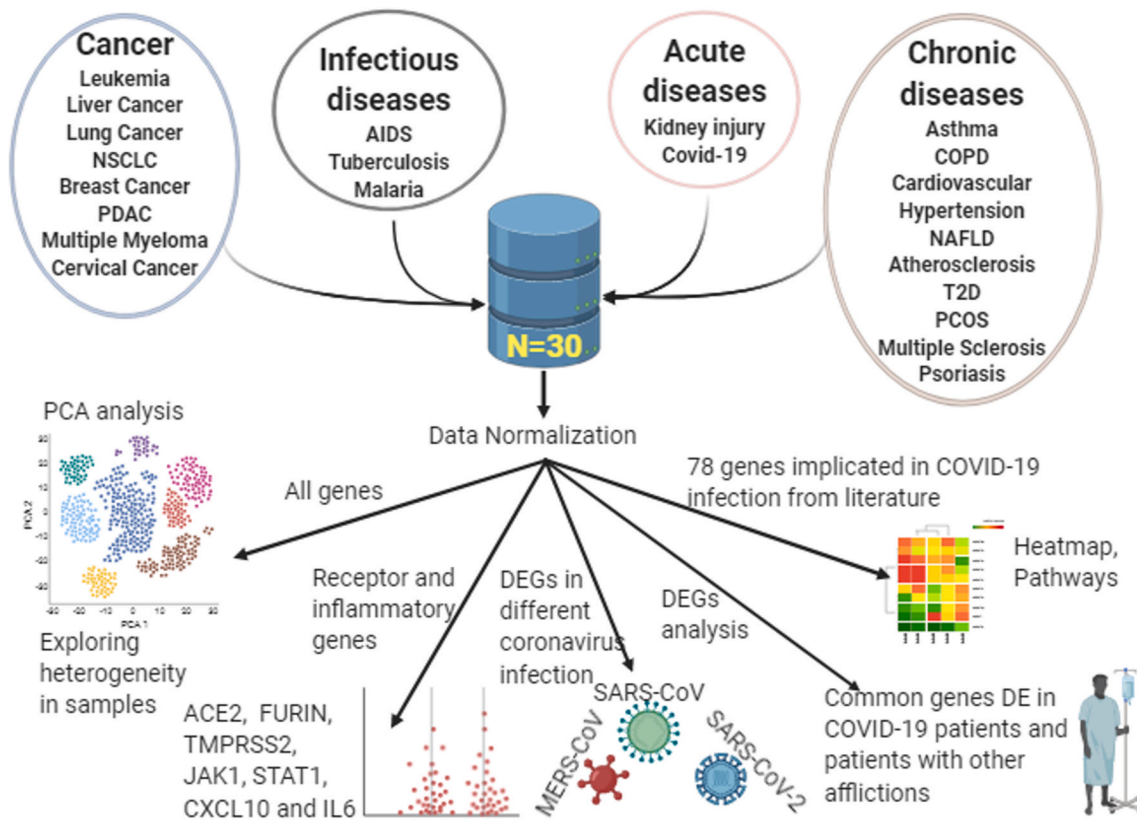


Fig. 1. Flow diagram of the study.

3. Results

3.1. Human genes implicated in the pathogenesis of COVID-19 are upregulated in leukemia, psoriasis, NAFLD, and type II diabetes cases

In leukemia and NAFLD condition, there were more than one dataset, namely one GSEid for samples and another GSEid for controls. In addition, in leukemia and breast cancer, the sample size of individual datasets was large. Therefore, we performed a principal component analysis (PCA) on the expression values of 10296 genes to explore the variability between datasets. We observed that the gene expression profile of datasets in a given disease correlated with each other, and each disease produced isolated galaxies of points closely spaced to each other (Fig. 2A). We then investigated the differential gene expression in a set of chronic, acute, and infectious disease conditions to identify the gene expression patterns that may induce susceptibility to SARS-CoV-2 infection. The molecular details of SARS-CoV-2 infection and spread are still under active research, and some steps in the pathogenesis of SARS-CoV-2 have been reported as either identical or similar to that of other pathogenic human coronaviruses (HCoVs), namely, SARS-CoV and MERS-CoV. Since gene expression pattern is characteristically correlated with the pathogenesis of diseases [19,20], we examined the expression patterns of human genes, which are implicated in the replication and

pathogenesis of SARS-CoV-2 or other HCoVs, in different disease conditions. To this end, we performed a literature mining exercise and identified 78 genes that were reported to have important implications in the entry and pathogenesis of HCoVs. These genes are enlisted in Supplementary Table 1. Some of these genes have been identified with key roles in promoting the pathogenesis of SARS-CoV-2, namely ACE2, FURIN, and TMPRSS2. The heatmap of log₂(FC) fold changes in expression values of these 78 genes, in all 30 disease cases including COVID-19, is shown in Fig. 2B. It is evident that several of these genes are upregulated in patients with SARS-CoV-2 infection and patients of all the studied subtypes of leukemia (hereafter, collectively referred to as leukemia; 45–50 genes), NAFLD (32 genes), psoriasis (22 genes), breast cancer (17 genes), cervical cancer (12 genes), NSCLC1 (7 genes), and type II diabetes liver (7 genes). It is noteworthy that the differential gene expression pattern was particularly pronounced in leukemia (log₂(FC) in the range 2–6) and NAFLD (log₂(FC) in the range 2–5).

Further, to investigate any prospective co-expression feature, we performed the co-expression analysis of 78 genes, which are implicated in the pathogenesis of coronaviruses, in these diseases. First, we examined the disease samples separately for each disease and identified the co-expressed genes in each case. Herein, we obtained a single module (turquoise) each for SARS-CoV-2, leukemia, psoriasis, PAH, and T2D Liver (Supplementary Figs. 1–5). 38 genes were observed to co-express

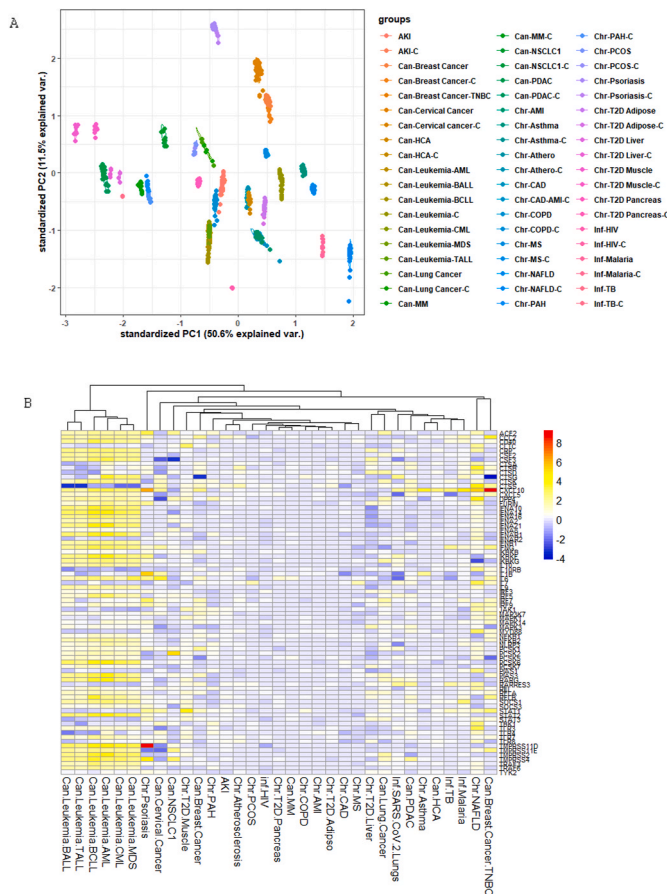


Fig. 2. (A) Principal Component Analysis of 10,296 gene expression values in the datasets used in this study for 30 disease conditions and their respective controls. Individual datasets are represented by separate points. To categorize and differentially color different disease types, we have inserted the prefixes “Can,” “Chr,” and “Inf” to identify the clusters of various types of cancer, chronic diseases, and infectious diseases, respectively. (B) Clustered heatmap depicting fold change ($\log_2(\text{FC})$) in the expression of 78 host genes in COVID-19 patients and in other 30 studied disease patients. (For interpretation of the references to colour in this figure legend, the reader is referred to the web version of this article.)

in each of these disease types (Supplementary Fig. 6). We obtained different hub genes in each of these diseases, namely, *MAPK1* in SARS-CoV-2, *PCSK6* in leukemia, *NFKB1* in PAH, *TYK2* in psoriasis, and *CTSD* in T2D liver (Supplementary Figs. 7–11). However, in the case of NAFLD, we did not obtain any module of co-expressed genes.

Thereafter, we performed another co-expression analysis using integrated $\log_2(\text{FC})$ values for SARS-CoV-2, leukemia (6 subtypes were considered separately), NAFLD, psoriasis, PAH, and T2D Liver (Supplementary Fig. 12). We obtained two modules with 62 and 16 genes, however, only one module was significant wherein *PCSK6* was identified as the hub gene (Supplementary Fig. 13). Pathway analysis with these genes showed the prominent enrichment of Toll-like receptor signaling, JAK/STAT signaling, TNF signaling and NF- κ B signaling pathways (Supplementary Table 2).

3.2. The expression of ACE2, FURIN, and TMPRSS2 is increased in leukemia, NAFLD, and psoriasis patients

The earliest steps in establishing COVID-19 include cellular entry of SARS-CoV-2, which is critically dependent on the host’s ACE2 receptor and serine proteases FURIN and TMPRSS2. ACE2 functions as the receptor for the entry of SARS-CoV-2 by binding to the viral spike protein,

whereas, the FURIN and TMPRSS2 proteases are essential for processing the spike protein that facilitates viral entry into the cells [21,22]. Therefore, we investigated the expression patterns of *ACE2*, *FURIN*, and *TMPRSS2* in the distinct disease cases (as identified in Fig. 2B), namely breast cancer, cervical cancer, leukemia, NAFLD, NSCLC1, psoriasis, and T2D. The expression of *ACE2* was upregulated in leukemia, psoriasis, NAFLD, lung cancer, breast cancer, and cervical cancer patients (Fig. 3A). The expression of *FURIN* was upregulated in leukemia, psoriasis, NAFLD, lung cancer, and in T2D liver whereas it was downregulated in breast cancer (Fig. 3B). We observed that *TMPRSS2* was upregulated in leukemia, lung cancer, and T2D, but it was downregulated in psoriasis, NAFLD, lung cancer, breast cancer, and cervical cancer (Fig. 3C). It is worthwhile to mention that after the interaction of the viral spike protein with ACE2 receptor, the host’s FURIN protease cleaves the spike protein at the interface of two subunits of the trimeric spike. Thus, the protease activity of FURIN is critical in promoting spike mediated entry of SARS-CoV-2 and it is also known to be crucial for protein processing in other infectious diseases and in cancer [23]. Similar to FURIN, the proteolytic cleavage of spike protein by TMPRSS2 is critical for its fusogenic activity.

3.3. Disease-associated dysregulation of innate and adaptive immune response in patients with other diseases

Following entry, the presence of viral RNA in cellular milieu evokes an immune response in the host. Apart from the receptors and proteases, the heatmap in Fig. 2B also shows the differential expression of genes, which are involved in the innate and acquired immune responses to SARS-CoV-2 invasion. The genes Interferon-alpha and Interferon-beta (*IFNA2*, *IFNA8*, *IFNA10*, *IFNA14*, *IFNA16*, *IFNA21*, and *IFNB1*) are the initial response elements of the innate immune signaling pathway. These responses activate several interferon-stimulated genes (ISGs) via JAK1/STAT1 pathway, which leads to early clearance of the viral load [24]. We prepared a heatmap of the $\log_2(\text{FC})$ of the expression of the interferons that were differentially expressed in any of the 30 diseases ($p < 0.05$, Fig. 4A). We also examined the expression of genes encoding cytokines that underlie the anti-viral immune responses, namely *IL6*, *CXCL10*, *JAK1*, and *STAT1* (Fig. 4B–E). The genes *IFNA2*, *IFNA8*, *IFNA10*, *IFNA14*, *IFNA16*, *IFNA21*, and *IFNB1* were upregulated in leukemia ($\log_2(\text{FC})$ ranged from 1.003 to 4.63) and in NAFLD ($\log_2(\text{FC})$ ranged from 1.009 to 1.93), whereas they were downregulated in T2D liver ($\log_2(\text{FC})$ ranged from -1.09 to -1.61). The expression of *JAK1* was slightly decreased ($\log_2(\text{FC})$ ranged from -0.63 to -0.94) in leukemia except in BCLL cases, whereas *STAT1* was slightly decreased in TALL ($\log_2(\text{FC})$ -0.41) and was unchanged in other types of leukemia. Both *JAK1* and *STAT1* were increased in NAFLD ($\log_2(\text{FC})$ ranged from 1.52 to 1.96) and in T2D muscles ($\log_2(\text{FC})$ ranged from 1.52 to 3.88). The initial interferon-mediated response is followed by a specific cell-mediated adaptive immune response to clear viral invasion. To this end, the cytokines *IL6* and *CXCL10* are produced by helper T cells and macrophages that promote the migration of immune cells to the site of infection. They are also associated with the cytokine storm observed in COVID-19 associated mortalities [25]. We observed that the expression of *IL6* and *CXCL10* was upregulated in leukemia ($\log_2(\text{FC})$ ranged from 1.92 to 3.55). But the expression of *IL6* was slightly decreased in NAFLD ($\log_2(\text{FC})$ -0.4). The expression of *CXCL10* was increased in NAFLD ($\log_2(\text{FC})$ 5.23) and PDAC ($\log_2(\text{FC})$ 2.095).

3.4. The patterns of differential gene expression are similar in SARS-CoV-2, leukemia, and NAFLD

We analyzed the expression pattern of 193 differentially expressed genes from 16 SARS-CoV-2 infected patients. Out of these 193 differentially expressed genes, we found that the expression values for only 182 genes were available in the datasets of all disease types included in our study. Therefore, we generated a clustered heatmap (Fig. 5A) and a

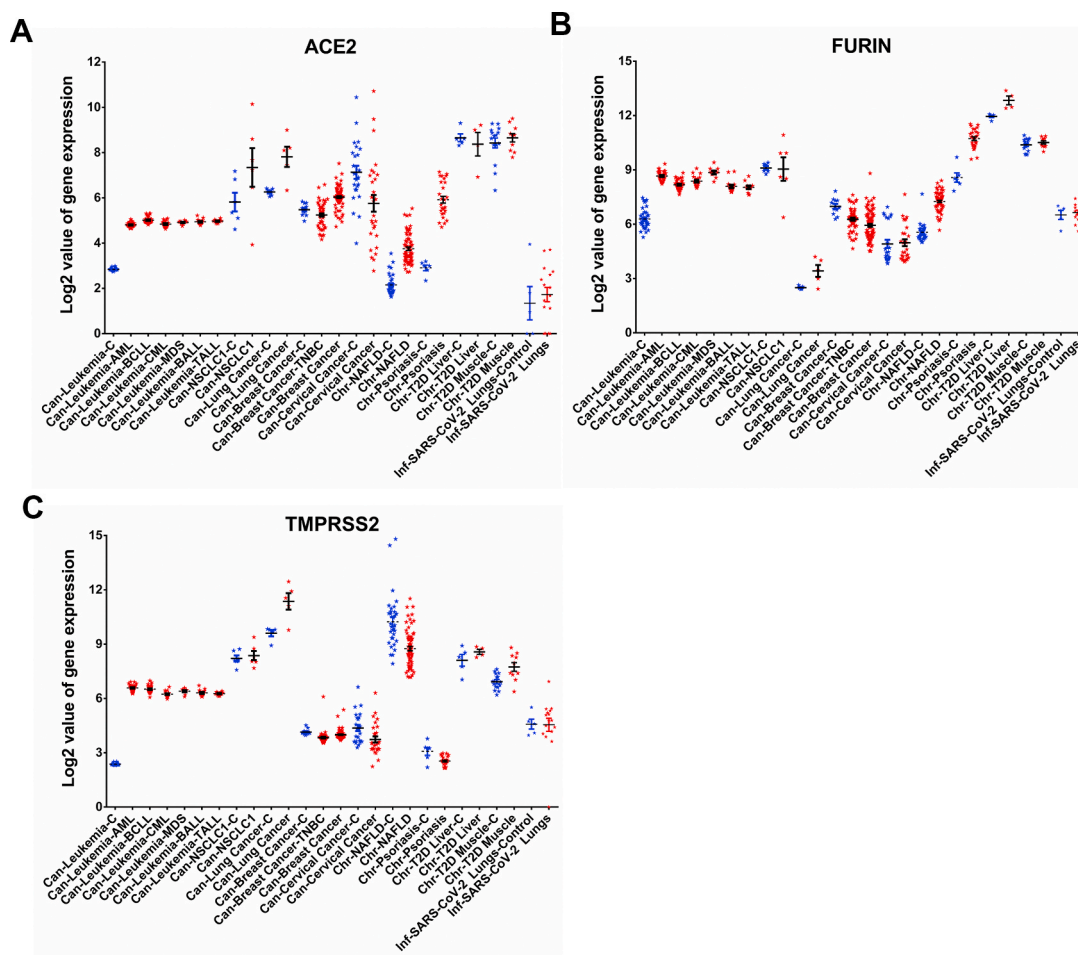


Fig. 3. Quantitative representation of gene expression values of (A) *ACE2*, (B) *FURIN*, and (C) *TMPRSS2* in patients and in their respective controls from 14 selected diseases wherein these genes were differentially regulated. Each point represents the gene expression values of controls (Blue) and of patients (Red) in individual disease cases. Bars depict standard error of mean. (For interpretation of the references to colour in this figure legend, the reader is referred to the web version of this article.)

scatter plot (Supplementary Fig. 14) depicting the expression of these 182 differentially expressed genes in 30 diseases and COVID-19 conditions. It is evident from the heatmap that the pattern of gene expression is similar in COVID-19 and PDAC, which are segregated together in the heatmap. Similarly, lung cancer and NSCLC also clustered together. Among the 161 genes upregulated in the lungs of COVID-19 patients ($\log_2(\text{FC})$ ranged from 1 to 3.45), 99–111 genes in leukemia ($\log_2(\text{FC})$ ranged from 1 to 5.86), 77 genes in NAFLD ($\log_2(\text{FC})$ ranged from 1 to 5.58), and 48 genes in psoriasis ($\log_2(\text{FC})$ ranged from 1 to 6.27) were upregulated. Pathways enrichment analysis of these 182 genes using DAVID [26,27] showed significant enrichment of the host's immune response to viral infection or infection-related immune pathways (Fig. 5B). Furthermore, we inferred the expression of 10 topmost significantly altered up- and down-regulated genes in COVID-19 patients and compared them to the disease cases showing similar pattern of gene expression, namely, T2D liver, NAFLD, psoriasis, leukemia, PDAC, lung cancer, NSCLC, TNBC, breast cancer, and cervical cancer (Supplementary Fig. 15). We observed that three genes, namely RAMP3 (Receptor Activity Modifying Protein 3), S100A2 (S100 Calcium Binding Protein A2), and CLCA2 (Chloride Channel Accessory 2) with a functional role in calcium signaling, were prominently upregulated in at least 7 studied disease types (including all subtypes of leukemia).

3.5. Pathogenic HCoVs differentially regulate the expression of *CARBONIC ANHYDRASE 11* and *CLUSTERIN* gene

We extended our investigation to identify the genes, whose expression may be commonly altered by the dreaded viruses of recent times. We analyzed the differential gene expression in patients with different viral infections, namely, SARS-CoV, SARS-CoV-2, MERS-CoV, H1N1, and other influenza viruses (H7N1, H5N1, H3N2, and H5N2). We observed that no gene was commonly altered in these viral infections (at a fold change $> \pm 2$, $p < 0.05$; Fig. 6A). However, two genes, namely *CARBONIC ANHYDRASE 11* (CA11) and *CLUSTERIN* (CLU) were commonly altered in the patients infected by pathogenic HCoVs, namely SARS-CoV, SARS-CoV-2, and MERS-CoV (at a fold change $> \pm 2$, $p < 0.05$; Fig. 6B). Based on the similarities in the patterns of differential gene expression in COVID-19 and other 30 diseases, we examined the expression of CA11 and CLU in breast cancer, cervical cancer, leukemia, NAFLD, NSCLC1, psoriasis, and T2D patients. The expression of CA11 was significantly upregulated in COVID-19 and leukemia (Fig. 6C), whereas CLU was upregulated in COVID-19 only (Fig. 6D).

4. Discussion

COVID-19 associated comorbidities have been reported with several acute and chronic diseases, which lead to poor outcomes. For instance, diabetes, cardiovascular disease, renal and pulmonary diseases, are frequently observed comorbidities that increase the case fatality rate in

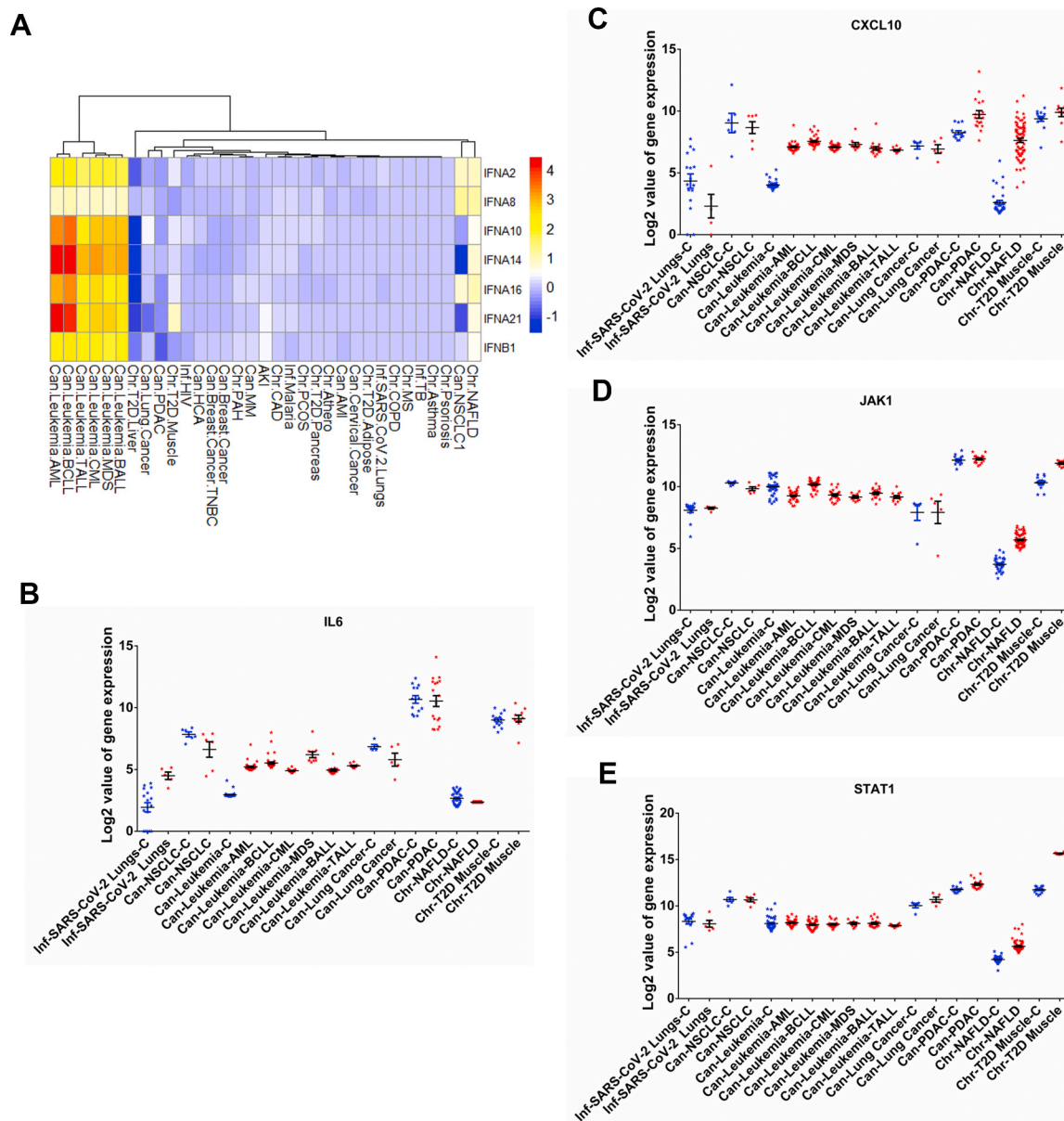


Fig. 4. (A) Clustered heatmap of log₂(FC) fold change values in the expression of genes encoding interferons that are differentially expressed in COVID-19 and 30 other studied disease patients. Quantification of (B) *IL6*, (C) *CXCL10*, (D) *JAK1*, and (E) *STAT1* expression in patients and in their respective controls from 12 selected diseases including COVID-19 wherein these genes were found to be differentially regulated. Each point represents fold changes from individual patient or control. Bars depict standard error of mean.

acute respiratory diseases caused by SARS-CoV [28], MERS-CoV [29, 30], and SARS-CoV-2. Our study revealed that the characteristic gene expression patterns in the disease cases, namely, leukemia, NAFLD, psoriasis, T2D, and PAH are highly similar to that of COVID-19. It is likely that the similarities in gene expression pattern offer a favorable environment to SARS-CoV-2 infection.

ACE2 is the functional receptor of three human infecting coronaviruses, namely NL-63, SARS-CoV, and SARS-CoV-2 [21,31]. Previous reports suggest that the expression of *ACE2* is moderate in lung alveolar epithelium cells, high in enterocytes of the small intestine, and to a lesser extent in the vascular endothelial and smooth muscle in several organs including kidney, liver, bone marrow, skin, and brain [32]. Through *ACE2*, these organs may provide an easy port of entry for SARS-CoV-2, and the gene expression data suggests that more severe symptoms could develop upon SARS-CoV-2 infection particularly in the respiratory tract and the gut. The degree of *ACE2* expression, in association with a 10–20 fold higher binding affinity of SARS-CoV-2 spike compared to

SARS-CoV spike, could underlie the efficient cellular entry and higher infectivity of SARS-CoV-2 compared to SARS-CoV [33,34]. We observed that the basal expression of *ACE2* was significantly high in many pathological conditions, namely leukemia, cancer of lungs, breasts, and cervix, NAFLD, psoriasis, and PAH. Hence, the increased number of available cellular receptors that facilitate viral entry can account for the increased susceptibility of these disease cases to SARS-CoV-2 infection.

Following the initial interaction of viral spike with *ACE2* receptors, the pre-activation of viral spike by cleavage at polybasic S1/S2 site in the spike is mediated by proprotein convertase *FURIN* that enables a second cleavage by the cellular serine protease *TMPRSS2*. Both these proteolytic cleavages are important in facilitating viral entry. Inactivation of either *FURIN* [22] or *TMPRSS2* [21] has been reported to inhibit cell-cell fusion and entry of SARS-CoV-2 in lung cells. Other cellular proteases such as *TMPRSS4* [35] *Cathepsin B* and *L* [34] may have a cumulative effect on the *FURIN*-mediated promotion of SARS-CoV-2 entry into enterocytes or liver or lungs cells. Except in CLL, BALL, and

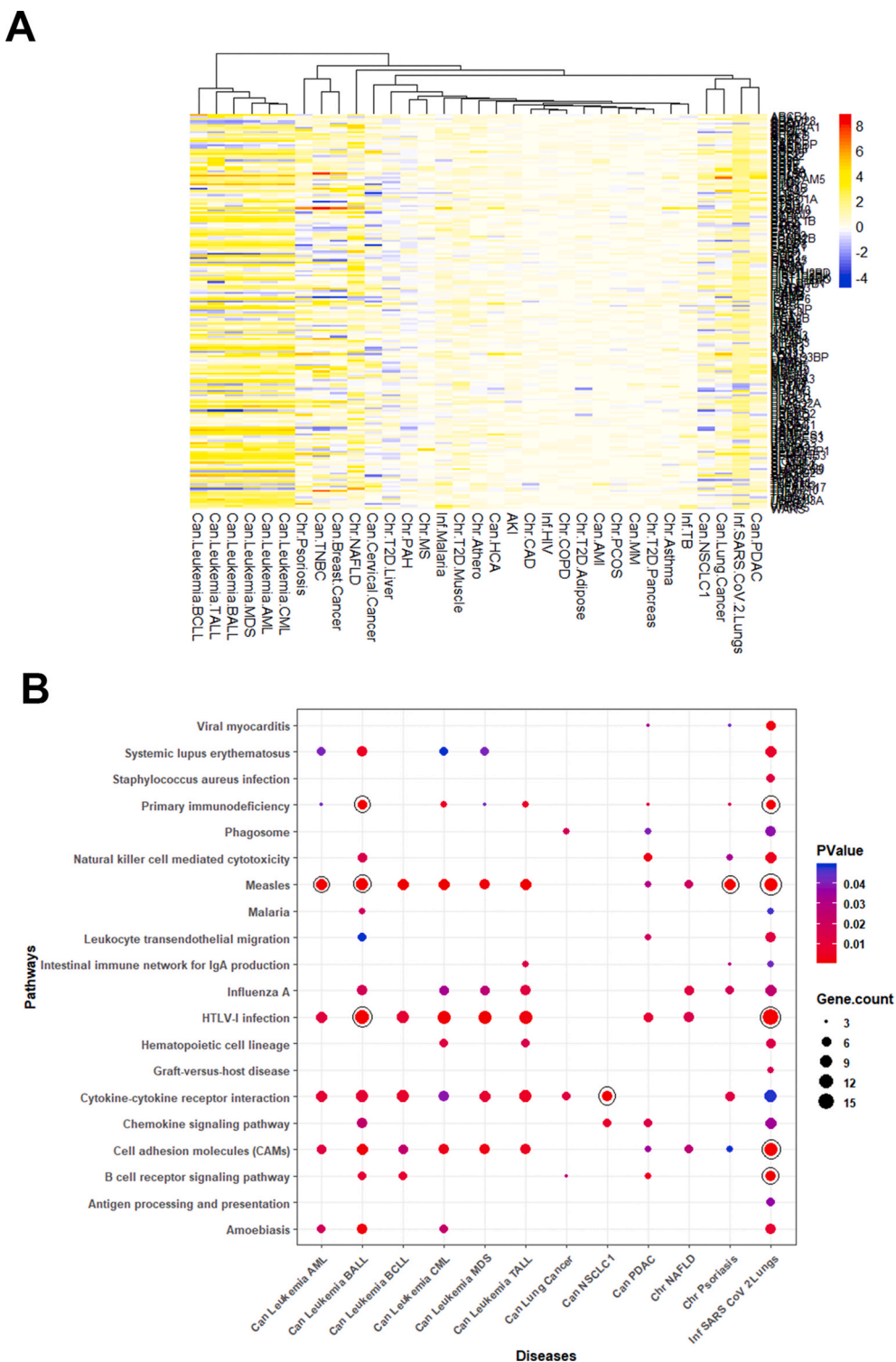


Fig. 5. (A) Clustered heat map of $\log_2(FC)$ fold change in the expression of 182 genes significantly altered in SARS-CoV-2 infected patients and in the 30 studied disease patients. (B) Bubble plot depicting the Pathways using 182 genes altered in COVID-19, leukemia, lung cancer, psoriasis, NAFLD, NSCLC, PDAC, and in T2D liver disease patients. Highly significant pathways in these diseases are highlighted with encircled bubbles according to p-adjusted values ($FDR < 0.05$).

TALL, wherein *CATHEPSIN A*, *B*, and *D* were downregulated, we observed that majority of the host proteases were highly upregulated in other subtypes of leukemia. Although cathepsins have an additive effect, they may not be indispensable for viral entry. Yet their increased expression along with that of *FURIN* and *TMPRSS2* can promote the processing of viral spike and enhance cellular entry of SARS-CoV-2 [21]. Taken together these data suggest that the patients of leukemia are

highly prone to SARS-CoV-2 infection. Similarly, the expression of *FURIN* was observed to be higher in NAFLD and psoriasis patients. Recently the abundance of either *FURIN* or *TMPRSS2* was shown to be sufficient in promoting the cellular entry of SARS-CoV-2 [21]. Although the relevant information on psoriasis is missing in the literature, Dong et al. (2020) have recently observed NAFLD comorbidity in COVID-19 patients [5]. Therefore, we propose that the increased expression of

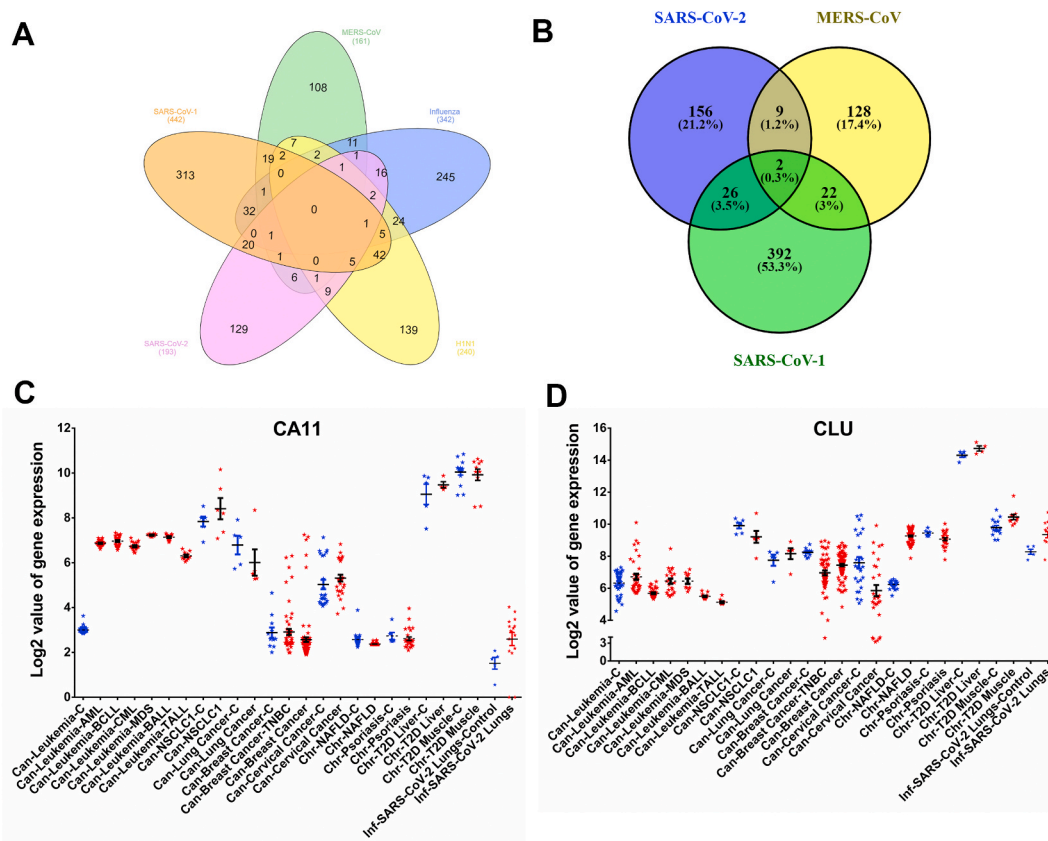


Fig. 6. Venn diagram depicting the number of differentially regulated genes in common to various viral infections, namely SARS-CoV, SARS-CoV-2, MERS-CoV, H1N1, and other influenza viruses (H7N1, H5N1, H3N2, and H5N2). (A) and to post-infection by pathogenic human infecting coronaviruses, namely SARS-CoV, SARS-CoV-2, and MERS-CoV (B). Quantification of expression of *Carbonic anhydrase 11* (CA11) (C) and *Clusterin* (Clu) (D) in patients and their respective controls from 14 selected diseases including COVID-19 wherein these genes were found to be differentially regulated. Each point represents fold changes from individual patients or controls. Bars depict standard error of mean.

ACE2 and *FURIN* could result in COVID-19 associated comorbidities. However, studies aimed at testing the redundancy of proteases are required to arrive at a definite conclusion.

Following the proteolytic cleavage of viral spike, the viral envelope fuses with host membrane and subsequently evokes the primary defense response of the host. This response is composed of the interferon-mediated innate immune response [36]. The production and binding of type I and type III interferons to their respective cellular receptors culminate into activating JAK1/STAT1 mediated transcription of several anti-viral interferon-stimulated genes [37]. It has been reported that the JAK1 deficient mice exhibit poor lymphoid development, and defective response to cytokines and interferons and die perinatally [38]. Similarly, mice with disrupted expression of STAT1 have compromised innate immunity [39] and are prone to viral infections [40]. Somatic mutations and dysregulation of JAK1 mediated signaling have been frequently observed in acute lymphoblastic leukemia [41,42]. Also, the deficiency of TYK2 (tyrosine kinase 2) in humans, which constitutes a key component of type I and type III interferon response, was shown to induce cytokine signaling defects and susceptibility to infection [43]. We observed that the expression of *IFNA2*, *IFNA8*, *IFNA10*, *IFNA14*, *IFNA16*, *IFNA21* and *IFNB1* were increased, whereas that of *JAK1*, *STAT1*, and *TYK2* did not change significantly in leukemia patients. Thus, the increased interferon response in leukemia patients may involve components other than JAK1, STAT1, and TYK2. In contrast, in NAFLD patients the increased expression of *JAK1* and *STAT1* corresponds well with the increased expression of the interferons encoding genes, namely, *IFNA2*, *IFNA8*, *IFNA10*, *IFNA14*, *IFNA16*, *IFNA21* and *IFNB1*. On the other hand, the expression of *JAK1* and *STAT1* decreased in T2D muscle and the expression of interferons decreased in T2D liver.

However, p-STAT1 levels must be quantified to conclusively reveal the correlation between STAT1 expression in COVID-19 associated comorbidities. The higher levels of interferons may be one of the reasons for the previously observed reports describing relatively milder symptomatic COVID-19 in CLL patients [44]. However, SARS-CoV-2 may use several escape or immune-suppression strategies including the formation of a replication organelle and 2'-O-methylated capping of viral RNA to proliferate despite of increased basal interferon levels in leukemia and NAFLD patients [45]. Thereafter, the specific adaptive immune response comes into effect for curbing the viral invasion. An optimal secretion of cytokines and chemokines (such as IL6 and CXCL10) from immune cells is essential to adjust the host's immune response against foreign invaders. However, the excess release of cytokines, also known as cytokine storm, is associated with an increased severity of disease and poorer outcomes in SARS-CoV [46,47] and SARS-CoV-2 [48] infected patients. Earlier, the inhibition of NF-κB mediated production of IL6 was found to increase the survival in SARS-CoV infected mice [49] and IL6 blockade has been thought of as a mechanism to manage cytokine storm and save COVID-19 patients [50]. We observed a higher basal expression of *CXCL10* in leukemia, NAFLD, and PDAC patients that may subsequently lead to cytokine storm upon SARS-CoV-2 infection. Recently Malard et al. (2020) have also reported that patients with hematologic malignancies are at higher risk of developing a severe form of COVID-19 [51]. Thus, we propose that the inhibitors of IL6 and CXCL10 could be examined for clinical interventions in leukemia and NAFLD patients who have been tested positive for SARS-CoV-2.

Furthermore, calcium signaling was found to be perturbed in COVID-19 and at least 6 other studied disease types including leukemia, NAFLD, and psoriasis that manifested in the form of altered expression of

RAMP3, S100A2, and CLCA2 genes. RAMP3 is a co-activator that targets the calcium-sensing receptor to cell surface [52,53]. CLCA2 regulates the calcium-activated chloride channel currents and enhances the store-operated cellular entry of calcium [54]. S100A2 encodes a cytoplasmic calcium-binding protein and is known to be dysregulated in human cancers [55]. Together, these three genes modulate the cellular calcium levels in response to various stimuli and were distinctly upregulated in leukemia, NAFLD, and psoriasis (Supplementary Fig. 1). Recently, Sun et al. (2020) showed that calcium channel blockers inhibit the replication of SARS-CoV-2 in the cellular milieu and reduce the COVID-19 associated case-fatality rate [56]. Thus, cellular calcium levels may play a significant role in inducing susceptibility to SARS-CoV-2 infection. Furthermore, we found that the expression of *CA11* and *CLU* genes were commonly altered in SARS-CoV, SARS-CoV-2, and MERS-CoV infected cases. These data indicate the uniqueness of the host gene expression patterns, thereby supporting the distinctive nature of these infections. Although *CA11* was upregulated in leukemia, no trend was observed in the expression of *CLU* in the studied disease types. As of now, no direct correlation has been identified between the expression of either *CA11* or *CLU* with the pathogenesis of SARS-CoV-2. However, several authors have recently identified that COVID-19 may lead to ketosis, ketoacidosis [57], and altered glucose metabolism [58]. Because *CA11* plays an important role in hepatic gluconeogenesis [59], it could be interesting to investigate the potential relationship between SARS-CoV-2 infection, differential *CA11* expression, and the onset of diabetes in COVID-19 patients.

Our study has few associated caveats. At first, we have selected the gene expression datasets from 30 diseases with strict criteria, namely, human samples with disease-specific tissues. The datasets were generated through expression profiling by array and the cases were devoid of any other treatments or afflictions. Given the reasonable number of samples used in these studies, we believe that our observations could be generally applicable. However, the limited sample size could impose limitations on confirming these observations in other samples including patients from other populations. This study concludes that the patients of leukemia are relatively more susceptible to SARS-CoV-2 infection followed by NAFLD, psoriasis, T2D, and PAH. It has been reported that STAT1 signaling promotes the proliferation of leukemia [60] and non-alcoholic steatohepatitis [61], and the inhibition of JAK/STAT signaling has shown protective activity in leukemia [60] and type II diabetes [62]. Complementarily, recent reports have observed down-regulation of STAT1 [63] and upregulation of CXCL10 [64] post SARS-CoV-2 infection. These reports suggest a potential target avenue [65]. Furthermore, it has been reported that the expression of IL-6 is upregulated in NAFLD [66], type II diabetes [67], and COVID-19 [68] patients. Previously, the IL-6 overexpression following SARS-CoV-2 infection was reported to occur via NF- κ B [46] and inhibition of NF- κ B signaling was reported to increase the survival in SARS-CoV infected mice [49]. Therefore, the strategy of inhibition of inflammatory cascade appears important for curbing SARS-CoV-2 infection with a concomitant increase in survival rates and for the added benefit of management of associated comorbidities. Therefore, our study indicates that disease-specific inhibition of IL6, CXCL10, JAK1, and STAT1 either alone or in various combinations could benefit in curbing COVID-19 associated comorbidities. Our report could support the healthcare systems across the globe in devising better management practices for preventing the complications of COVID-19 associated comorbidities.

Author contribution

MKS, AM, and AC: Conceptualization, Data curation, Formal analysis, Investigation, methodology, validation, visualization, writing – original draft, review & editing. **SJ:** Investigation, methodology, validation, visualization, writing – original draft, review & editing. **SR:** Data curation, Funding acquisition, Project administration, supervision, writing – review & editing.

Funding statement

No disclosures to make.

Declaration of competing interest

Authors declare that they have no conflict of interest.

Acknowledgment

MKS and AC acknowledge CSIR for a research fellowship, AM acknowledges ICMR for a research fellowship. SR acknowledges financial support from Department of Biotechnology, India [Grant No. BT/PR16472/BID/7/629/2016].

Appendix A. Supplementary data

Supplementary data to this article can be found online at <https://doi.org/10.1016/j.compbmed.2021.104219>.

References

- [1] W.J. Guan, W.H. Liang, Y. Zhao, H.R. Liang, Z.S. Chen, Y.M. Li, X.Q. Liu, R.C. Chen, C.L. Tang, T. Wang, C.Q. Ou, L. Li, P.Y. Chen, L. Sang, W. Wang, J.F. Li, C.C. Li, L. M. Ou, B. Cheng, S. Xiong, Z.Y. Ni, J. Xiang, Y. Hu, L. Liu, H. Shan, C.L. Lei, Y. X. Peng, L. Wei, Y. Liu, Y.H. Hu, P. Peng, J.M. Wang, J.Y. Liu, Z. Chen, G. Li, Z. J. Zheng, S.Q. Qiu, J. Luo, C.J. Ye, S.Y. Zhu, L.L. Cheng, F. Ye, S.Y. Li, J.P. Zheng, N.F. Zhang, N.S. Zhong, J.X. He, C. China Medical Treatment, Expert Group for, Comorbidity and its impact on 1590 patients with COVID-19 in China: a nationwide analysis, *Eur. Respir. J.* 55 (2020).
- [2] N. Chen, M. Zhou, X. Dong, J. Qu, F. Gong, Y. Han, Y. Qiu, J. Wang, Y. Liu, Y. Wei, J. Xia, T. Yu, X. Zhang, L. Zhang, Epidemiological and clinical characteristics of 99 cases of 2019 novel coronavirus pneumonia in Wuhan, China: a descriptive study, *Lancet* 395 (2020) 507–513.
- [3] F. Yang, S. Shi, J. Zhu, J. Shi, K. Dai, X. Chen, Clinical characteristics and outcomes of cancer patients with COVID-19, *J. Med. Virol.* 92 (10) (2020) 2067–2073.
- [4] W. Li, D. Wang, J. Guo, G. Yuan, Z. Yang, R.P. Gale, Y. You, Z. Chen, S. Chen, C. Wan, X. Zhu, W. Chang, L. Sheng, H. Cheng, Y. Zhang, Q. Li, J. Qin, A. Hubei Anti-Cancer, L. Meng, Q. Jiang, COVID-19 in persons with chronic myeloid leukaemia, *Leukemia* (2020).
- [5] D. Ji, E. Qin, J. Xu, D. Zhang, G. Cheng, Y. Wang, G. Lau, Non-alcoholic fatty liver diseases in patients with COVID-19: a retrospective study, *J. Hepatol.* 73 (2) (2020) 451–453.
- [6] J.L. Blanco, J. Ambrosioni, F. Garcia, E. Martinez, A. Soriano, J. Mallolas, J. M. Miro, C.-i.H. Investigators, COVID-19 in patients with HIV: clinical case series, *Lancet HIV* 7 (2020) e314–e316.
- [7] M.E. Dolan, D.P. Hill, G. Mukherjee, M.S. McAndrews, E.J. Chesler, J.A. Blake, Investigation of COVID-19 comorbidities reveals genes and pathways coincident with the SARS-CoV-2 viral disease, *Sci. Rep.* 10 (2020) 20848.
- [8] R. Edgar, M. Domrachev, A.E. Lash, Gene Expression Omnibus: NCBI gene expression and hybridization array data repository, *Nucleic Acids Res.* 30 (2002) 207–210.
- [9] C.J. Walsh, P. Hu, J. Batt, C.C. Santos, Microarray meta-analysis and cross-platform normalization: integrative genomics for robust biomarker discovery, *Microarrays (Basel)* 4 (2015) 389–406.
- [10] J.S. Hamid, P. Hu, N.M. Roslin, V. Ling, C.M. Greenwood, J. Beyene, Data integration in genetics and genomics: methods and challenges, *Hum. Genom. Proteomics* (2009) 2009.
- [11] R.C. Team, R: A Language and Environment for Statistical Computing, 2013. Vienna, Austria.
- [12] G.K. Smyth, *Limma: Linear Models for Microarray Data*, Bioinformatics and Computational Biology Solutions Using R and Bioconductor, Springer, 2005, pp. 397–420.
- [13] P. Langfelder, S. Horvath, WGCNA: an R package for weighted correlation network analysis, *BMC Bioinf.* 9 (2008) 559.
- [14] B. Ripley, B. Venables, D.M. Bates, K. Hornik, A. Gebhardt, D. Firth, M.B. Ripley, Package ‘mass’, *Cran R*, 2013, p. 538.
- [15] V.Q. Vu, ggbplot: a ggplot2 based biplot, *R package* (2011) 342.
- [16] R. Kolde, M.R. Kolde, Package ‘pheatmap’, *R Package* 1 (2015) 790.
- [17] D.W. Huang, B.T. Sherman, Q. Tan, J. Kir, D. Liu, D. Bryant, Y. Guo, R. Stephens, M.W. Baseler, H.C. Lane, DAVID Bioinformatics Resources: expanded annotation database and novel algorithms to better extract biology from large gene lists, *Nucleic Acids Res.* 35 (2007) W169–W175.
- [18] M.S. Cline, M. Smoot, E. Cerami, A. Kuchinsky, N. Landys, C. Workman, R. Christmas, I. Avila-Campilo, M. Creech, B. Gross, Integration of biological networks and gene expression data using Cytoscape, *Nat. Protoc.* 2 (2007) 2366.
- [19] W. Ning, C.J. Li, N. Kaminski, C.A. Feghali-Bostwick, S.M. Alber, Y.P. Di, S. L. Otterbein, R. Song, S. Hayashi, Z. Zhou, D.J. Pinsky, S.C. Watkins, J.M. Pilewski, F.C. Sciruba, D.G. Peters, J.C. Hogg, A.M. Choi, Comprehensive gene expression

- profiles reveal pathways related to the pathogenesis of chronic obstructive pulmonary disease, *Proc. Natl. Acad. Sci. U. S. A.* 101 (2004) 14895–14900.
- [20] T.I. Lee, R.A. Young, Transcriptional regulation and its misregulation in disease, *Cell* 152 (2013) 1237–1251.
- [21] M. Hoffmann, H. Kleine-Weber, S. Schroeder, N. Kruger, T. Herrler, S. Erichsen, T. S. Schiergens, G. Herrler, N.H. Wu, A. Nitsche, M.A. Muller, C. Drosten, S. Pohlmann, SARS-CoV-2 cell entry depends on ACE2 and TMPRSS2 and is blocked by a clinically proven protease inhibitor, *Cell* 181 (2020) 271–280, e278.
- [22] M. Hoffmann, H. Kleine-Weber, S. Pohlmann, A multibasic cleavage site in the spike protein of SARS-CoV-2 is essential for infection of human lung cells, *Mol. Cell* 78 (2020) 779–784, e775.
- [23] E. Braun, D. Sauter, Furin-mediated protein processing in infectious diseases and cancer, *Clin Transl Immunology* 8 (2019), e1073.
- [24] C. Le Page, P. Genin, M.G. Baines, J. Hiscott, Interferon activation and innate immunity, *Rev. Immunogenet.* 2 (2000) 374–386.
- [25] N. Zhang, Y.D. Zhao, X.M. Wang, CXCL10 an important chemokine associated with cytokine storm in COVID-19 infected patients, *Eur. Rev. Med. Pharmacol. Sci.* 24 (2020) 7497–7505.
- [26] W. Huang da, B.T. Sherman, R.A. Lempicki, Systematic and integrative analysis of large gene lists using DAVID bioinformatics resources, *Nat. Protoc.* 4 (2009) 44–57.
- [27] W. Huang da, B.T. Sherman, R.A. Lempicki, Bioinformatics enrichment tools: paths toward the comprehensive functional analysis of large gene lists, *Nucleic Acids Res.* 37 (2009) 1–13.
- [28] E.H. Lau, C.A. Hsiung, B.J. Cowling, C.H. Chen, L.M. Ho, T. Tsang, C.W. Chang, C. A. Donnelly, G.M. Leung, A comparative epidemiologic analysis of SARS in Hong Kong, Beijing and Taiwan, *BMC Infect. Dis.* 10 (2010) 50.
- [29] K.A. Kulcsar, C.M. Coleman, S.E. Beck, M.B. Frieman, Comorbid diabetes results in immune dysregulation and enhanced disease severity following MERS-CoV infection, *JCI Insight* (2019) 4.
- [30] Y.M. Yang, C.Y. Hsu, C.C. Lai, M.F. Yen, P.S. Wikramaratna, H.H. Chen, T.H. Wang, Impact of comorbidity on fatality rate of patients with Middle East respiratory syndrome, *Sci. Rep.* 7 (2017) 11307.
- [31] I. Glowacka, S. Bertram, P. Herzog, S. Pfeifferle, I. Steffen, M.O. Muench, G. Simmons, H. Hofmann, T. Kuri, F. Weber, J. Eichler, C. Drosten, S. Pohlmann, Differential downregulation of ACE2 by the spike proteins of severe acute respiratory syndrome coronavirus and human coronavirus NL63, *J. Virol.* 84 (2010) 1198–1205.
- [32] I. Hamming, W. Timens, M.L. Bulthuis, A.T. Lely, G. Navis, H. van Goor, Tissue distribution of ACE2 protein, the functional receptor for SARS coronavirus. A first step in understanding SARS pathogenesis, *J. Pathol.* 203 (2004) 631–637.
- [33] M. Liu, T. Wang, Y. Zhou, Y. Zhao, Y. Zhang, J. Li, Potential role of ACE2 in coronavirus disease 2019 (COVID-19) prevention and management, *J Transl Int Med* 8 (2020) 9–19.
- [34] J. Shang, Y. Wan, C. Luo, G. Ye, Q. Geng, A. Auerbach, F. Li, Cell entry mechanisms of SARS-CoV-2, *Proc. Natl. Acad. Sci. U. S. A.* 117 (2020) 11727–11734.
- [35] R. Zang, M.F. Gomez Castro, B.T. McCune, Q. Zeng, P.W. Rothlauf, N.M. Sonnek, Z. Liu, K.F. Brulois, X. Wang, H.B. Greenberg, M.S. Diamond, M.A. Ciorba, S.P. J. Whelan, S. Ding, TMPRSS2 and TMPRSS4 promote SARS-CoV-2 infection of human small intestinal enterocytes, *Sci Immunol* 5 (2020).
- [36] X. Lei, X. Dong, R. Ma, W. Wang, X. Xiao, Z. Tian, C. Wang, Y. Wang, L. Li, L. Ren, F. Guo, Z. Zhao, Z. Zhou, Z. Xiang, J. Wang, Activation and evasion of type I interferon responses by SARS-CoV-2, *Nat. Commun.* 11 (2020) 3810.
- [37] A. Majoros, E. Platanitis, E. Kernbauer-Holz, F. Rosebrock, M. Muller, T. Decker, Canonical and non-canonical aspects of JAK-STAT signaling: lessons from interferons for cytokine responses, *Front. Immunol.* 8 (2017) 29.
- [38] P. Igaz, S. Toth, A. Falus, Biological and clinical significance of the JAK-STAT pathway; lessons from knockout mice, *Inflamm. Res.* 50 (2001) 435–441.
- [39] J.E. Durbin, R. Hackenmiller, M.C. Simon, D.E. Levy, Targeted disruption of the mouse Stat1 gene results in compromised innate immunity to viral disease, *Cell* 84 (1996) 443–450.
- [40] S.R. Jung, T.M. Ashhurst, P.K. West, B. Viengkhou, N.J.C. King, I.L. Campbell, M. J. Hofer, Contribution of STAT1 to innate and adaptive immunity during type I interferon-mediated lethal virus infection, *PLoS Pathog.* 16 (2020), e1008525.
- [41] E. Flex, V. Petrangeli, L. Stella, S. Chiaretti, T. Hornakova, L. Knoops, C. Ariola, V. Fodale, E. Clappier, F. Paoloni, S. Martinelli, A. Fragale, M. Sanchez, S. Tavoraro, M. Messina, G. Cazzaniga, A. Camera, G. Pizzolo, A. Tornesello, M. Vignetti, A. Battistini, H. Cave, B.D. Gelb, J.C. Renaud, A. Biondi, S. N. Constantinescu, R. Foa, M. Tartaglia, Somatically acquired JAK1 mutations in adult acute lymphoblastic leukemia, *J. Exp. Med.* 205 (2008) 751–758.
- [42] T. Hornakova, J. Staerk, Y. Royer, E. Flex, M. Tartaglia, S.N. Constantinescu, L. Knoops, J.C. Renaud, Acute lymphoblastic leukemia-associated JAK1 mutants activate the Janus kinase/STAT pathway via interleukin-9 receptor alpha homodimers, *J. Biol. Chem.* 284 (2009) 6773–6781.
- [43] Y. Minegishi, M. Saito, T. Morio, K. Watanabe, K. Agematsu, S. Tsuchiya, H. Takada, T. Hara, N. Kawamura, T. Ariga, H. Kaneko, N. Kondo, I. Tsuge, A. Yachie, Y. Sakiyama, T. Iwata, F. Bessho, T. Ohishi, K. Joh, K. Imai, K. Kogawa, M. Shinohara, M. Fujieda, H. Wakiguchi, S. Pasic, M. Abinun, H.D. Ochs, E. D. Renner, A. Jansson, B.H. Belohradsky, A. Metin, N. Shimizu, S. Mizutani, T. Miyawaki, S. Nonoyama, H. Karasuyama, Human tyrosine kinase 2 deficiency reveals its requisite roles in multiple cytokine signals involved in innate and acquired immunity, *Immunity* 25 (2006) 745–755.
- [44] T. Baumann, J. Delgado, E. Montserrat, CLL and COVID-19 at the Hospital Clinic of Barcelona: an Interim Report, 2020. Leukemia.
- [45] M. Kikkert, Innate immune evasion by human respiratory RNA viruses, *J Innate Immun* 12 (2020) 4–20.
- [46] W. Wang, L. Ye, L. Ye, B. Li, B. Gao, Y. Zeng, L. Kong, X. Fang, H. Zheng, Z. Wu, Y. She, Up-regulation of IL-6 and TNF-alpha induced by SARS-coronavirus spike protein in murine macrophages via NF-kappaB pathway, *Virus Res.* 128 (2007) 1–8.
- [47] C. Castilletti, L. Bordi, E. Lalle, G. Rozera, F. Poccia, C. Agrati, I. Abbate, M. R. Capobianchi, Coordinate induction of IFN-alpha and -gamma by SARS-CoV also in the absence of virus replication, *Virology* 341 (2005) 163–169.
- [48] C. Zhang, Z. Wu, J.W. Li, H. Zhao, G.Q. Wang, Cytokine release syndrome in severe COVID-19: interleukin-6 receptor antagonist tocilizumab may be the key to reduce mortality, *Int. J. Antimicrob. Agents* 55 (2020) 105954.
- [49] M.L. DeDiego, J.L. Nieto-Torres, J.A. Regla-Nava, J.M. Jimenez-Guardeno, R. Fernandez-Delgado, C. Fett, C. Castano-Rodriguez, S. Perlman, L. Enjuanes, Inhibition of NF-kappaB-mediated inflammation in severe acute respiratory syndrome coronavirus-infected mice increases survival, *J. Virol.* 88 (2014) 913–924.
- [50] B. Liu, M. Li, Z. Zhou, X. Guan, Y. Xiang, Can we use interleukin-6 (IL-6) blockade for coronavirus disease 2019 (COVID-19)-induced cytokine release syndrome (CRS)? *J. Autoimmun.* 111 (2020) 102452.
- [51] F. Malard, A. Genthon, E. Brissot, Z. van de Wyngaert, Z. Marjanovic, S. Ikhlef, A. Banet, S. Lapusan, S. Sestilli, E. Corre, A. Paviglianiti, R. Adaeva, F. M. Hammedi-Bouzina, M. Labopin, O. Legrand, R. Dulery, M. Mohty, COVID-19 outcomes in patients with hematologic disease, *Bone Marrow Transplant* (2020).
- [52] T. Bouschet, S. Martin, J.M. Henley, Receptor-activity-modifying proteins are required for forward trafficking of the calcium-sensing receptor to the plasma membrane, *J. Cell Sci.* 118 (2005) 4709–4720.
- [53] L. D'Souza-Li, The calcium-sensing receptor and related diseases, *Arq. Bras. Endocrinol. Metabol.* 50 (2006) 628–639.
- [54] A. Sharma, G. Ramena, Y. Yin, L. Premkumar, R.C. Elble, CLCA2 is a positive regulator of store-operated calcium entry and TMEM16A, *PLoS One* 13 (2018), e0196512.
- [55] A.R. Bresnick, D.J. Weber, D.B. Zimmer, S100 proteins in cancer, *Nat. Rev. Canc.* 15 (2015) 96–109.
- [56] L. Zhang, Y. Sun, H.-L. Zeng, Y. Peng, X. Jiang, W.-J. Shang, Y. Wu, S. Li, Y.-L. Zhang, L. Yang, Calcium Channel Blocker Amlodipine Besylate Is Associated with Reduced Case Fatality Rate of COVID-19 Patients with Hypertension, *medRxiv*, 2020.
- [57] J. Li, X. Wang, J. Chen, X. Zuo, H. Zhang, A. Deng, COVID-19 infection may cause ketosis and ketoacidosis, *Diabetes Obes Metab* (2020).
- [58] F. Rubino, S.A. Amiel, P. Zimmet, G. Alberti, S. Bornstein, R.H. Eckel, G. Mingrone, B. Boehm, M.E. Cooper, Z. Chai, S. Del Prato, L. Ji, D. Hopkins, W.H. Herman, K. Khunti, J.C. Mbanya, E. Renard, New-onset diabetes in Covid-19, *N Engl J Med* (2020).
- [59] I.S. Ismail, The role of carbonic anhydrase in hepatic glucose production, *Curr. Diabetes Rev.* 14 (2018) 108–112.
- [60] J. Habel, L. Arnold, Y. Chen, M. Mollmann, K. Bruderek, S. Brandau, U. Duhrsen, M. Hanoun, Inflammation-driven activation of JAK/STAT signaling reversibly accelerates acute myeloid leukemia in vitro, *Blood Adv.* 4 (2020) 3000–3010.
- [61] M. Grohmann, F. Wiede, G.T. Dodd, E.N. Gurzov, G.J. Ooi, T. Butt, A.A. Rasmiena, S. Kaur, T. Gulati, P.K. Goh, A.E. Treloar, S. Archer, W.A. Brown, M. Muller, M. J. Watt, O. Ohara, C.A. McLean, T. Tiganis, Obesity drives STAT-1-dependent NASH and STAT-3-dependent HCC, *Cell* 175 (2018) 1289–1306 e1220.
- [62] F.M. Couto, A.H. Minn, C.A. Pise-Masison, M. Radonovic, J.N. Brady, M. Hanson, L.A. Fernandez, P. Wang, C. Kendziorski, A. Shalev, Exenatide blocks JAK1-STAT1 in pancreatic beta cells, *Metabolism* 56 (2007) 915–918.
- [63] L. Miorin, T. Kehrer, M.T. Sanchez-Aparicio, K. Zhang, P. Cohen, R.S. Patel, A. Cupic, T. Makio, M. Mei, E. Moreno, O. Danziger, K.M. White, R. Rathnasinghe, M. Uccellini, S. Gao, T. Aydiillo, I. Mena, X. Yin, L. Martin-Sancho, N.J. Krogan, S. K. Chanda, M. Schotsaert, R.W. Wozniak, Y. Ren, B.R. Rosenberg, B.M.A. Fontoura, A. Garcia-Sastre, SARS-CoV-2 Orf 6 hijacks Nup98 to block STAT nuclear import and antagonize interferon signaling, *Proc. Natl. Acad. Sci. U. S. A.* 117 (2020) 28344–28354.
- [64] M. Blot, M. Jacquier, L.S. Aho Glele, G. Beltramo, M. Nguyen, P. Bonniaud, S. Prin, P. Andreu, B. Bouhemad, J.B. Bour, C. Binquet, L. Piroth, J.P. Pais de Barros, D. Masson, J.P. Quenot, P.E. Charles, g. Pneumochondrie study, CXCL10 could drive longer duration of mechanical ventilation during COVID-19 ARDS, *Crit. Care* 24 (2020) 632.
- [65] Y.S. Chang, B.H. Ko, J.C. Ju, H.H. Chang, S.H. Huang, C.W. Lin, SARS unique domain (SUD) of severe acute respiratory syndrome coronavirus induces NLRP3 inflammasome-dependent CXCL10-mediated pulmonary inflammation, *Int. J. Mol. Sci.* 21 (2020).
- [66] S.K. Das, V. Balakrishnan, Role of cytokines in the pathogenesis of non-alcoholic fatty liver disease, *Indian J. Clin. Biochem.* 26 (2011) 202–209.
- [67] O.P. Kristiansen, T. Mandrup-Poulsen, Interleukin-6 and diabetes: the good, the bad, or the indifferent? *Diabetes* 54 (Suppl 2) (2005) S114–S124.
- [68] E. Grifoni, A. Valoriani, F. Cei, R. Lamanna, A.M.G. Gelli, B. Ciambotti, V. Vannucchi, F. Moroni, L. Pelagatti, R. Tarquini, G. Landini, S. Vanni, L. Masotti, Interleukin-6 as prognosticator in patients with COVID-19, *J. Infect.* 81 (2020) 452–482.